NJC

ROYAL SOCIETY OF CHEMISTRY

PAPER

View Article Online
View Journal | View Issue

Cite this: *New J. Chem.*, 2021, **45**, 5428

Enantioseparation and determination of orphenadrine in rat plasma and its application to a stereoselective pharmacokinetic study

Yanru Liu, Yushan Ding, Yongbo Song* and Xingjie Guo*

Received 9th December 2020,
Accepted 12th February 2021

DOI: 10.1039/d0nj06005d

rsc.li/njc

A simple, sensitive, and enantioselective HPLC-MS/MS method has been developed for the determination of orphenadrine (ORP) enantiomers in rat plasma for the first time. The method used diphenhydramine as the internal standard (IS), and plasma samples were extracted by liquid–liquid extraction with satisfactory recovery. Chiral separation of the ORP enantiomers was obtained on a Chiralcel OD-RH column (150 mm × 4.6 mm, 5 μm). The mobile phase consists of acetonitrile–ammonium bicarbonate buffer (30 mM, pH 9.0) (80 : 20, v/v). Sufficient resolution (R_s = 3.562) was achieved in a short analysis time (7 min). The multiple reaction monitoring (MRM) mode was used for the detection of ORP enantiomers and IS. The transitions of *m/z* 270.0 → 181.1 and 256.2 → 167.1 were chosen for monitoring the ORP enantiomers and IS, respectively. Linearity was confirmed in the range of 0.1–50.0 ng mL^{-1} with the lower limit of quantification of 0.1 ng mL^{-1} for both ORP enantiomers in plasma. After validation, the method was applied to the enantioselective pharmacokinetic study of ORP enantiomers in rat plasma following oral administration of 10 mg kg^{-1} racemic ORP. Significant differences ($P < 0.05$) of ORP enantiomers were observed in pharmacokinetic parameters including C_{max}, AUC, $t_{1/2}$, CL, V_d, MRT, and VRT, which indicated that enantioselective pharmacokinetic behavior of ORP enantiomers was present in rats.

1. Introduction

It is well known that enantiomers of one chiral drug always show different pharmacological activities or toxicities due to the specific enantioselective interactions with receptors, enzymes, or other biological macromolecules.[1–8] Therefore, the stereoselective study of the chiral drugs is crucial and an efficient enantioselective bioanalytical method is a pivotal way to elucidate the absorption, distribution, metabolism, and excretion (ADME) of chiral drugs.

Orphenadrine (*N*,*N*-dimethyl-2(*o*-methyl-alpha-phenylbenzyloxy)-ethylamine; ORP, Fig. 1) is a chiral anticholinergic drug belonging to the ethanolamine antihistamine class.[9] It is widely accepted as a skeletal muscle relaxant in the form of the racemate and is used as a therapeutic agent in the treatment of Parkinson's disease and neuroleptic syndrome.[10] In terms of the chemical structure, ORP contains one asymmetric carbon and possesses two enantiomers. Different chiral selectors have been applied for the chiral separation of ORP enantiomers under suitable capillary electrophoresis (CE) conditions. Namely, ORP enantiomers can be separated by CE using different chiral selectors including human serum albumin (HSA),[11,12] sulfated-β-CD,[13–15] hydroxypropyl-γ-CD,[16] and hydroxypropyl-α-CD.[17] Furthermore, high-performance liquid chromatography (HPLC) with chiral stationary phase (CSP) methods were proved to be effective and convenient for chiral separation and analysis.[18–20] Among them, macrocyclic glycopeptides and polysaccharide derivatives have been investigated to achieve higher selectivities for difficult and important chiral separations.[21–23] For example, the enantioseparation of ORP has been achieved on immobilized cellulose tris (3,5-dimethylphenylcarbamate) and macrocyclic glycopeptide based CSPs (VancoShell and NicoShell) in reversed-phase mode.[24,25] And thus, Kummer *et al.* have proposed a chiral LC method with a Phenomenex® Lux Cellulose-1 column for the determination of the ORP enantiomers in commercially available tablets.[26]

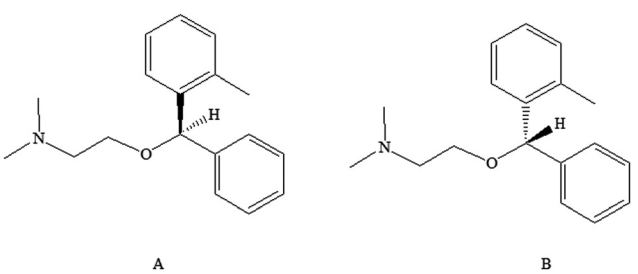

Fig. 1 Chemical structures of *R*-ORP (A) and *S*-ORP (B).

School of Pharmacy, Shenyang Pharmaceutical University, No. 103 Wenhua Road, Shenhe District, Shenyang, 110016, Liaoning Province, P. R. China. E-mail: gxjhyz@gmail.com, songyongbo@syphu.edu.cn; Fax: +86-24-23986285, +86-24-23986285

Enantioselectivity behavior of the two ORP enantiomers in human plasma protein binding has been reported.[11,27] However, to date, there is no information available on the enantioselective pharmacokinetics study of ORP enantiomers, and the pharmacology and toxicology of the two isomers are still unknown. Hence, in order to ensure the safety of administration in clinical applications, and promote the development of a single enantiomer, the development of an enantioselective pharmacokinetics approach for ORP is desperately needed.

Many liquid chromatography (LC),[28,29] gas chromatography-mass spectrometry (GC-MS),[30,31] liquid chromatography-mass spectrometry (LC-MS and LC-MS/MS),[32,33] and capillary electrophoresis (CE)[34] methods have been developed for the determination of ORP in pharmaceutical preparations and biological fluids. In particular, the combination of HPLC and tandem MS detection with high sensitivity allows for a simple and fast sample pretreatment procedure, which could greatly reduce the analysis time. However, the HPLC-MS/MS method for the enantioselective pharmacokinetic determination of ORP enantiomers has not been reported.

In order to study the stereoselective pharmacokinetics of *R*- and *S*-ORP enantiomers, coated cellulose tris(3,5-dimethylphenylcarbamate) CSP (Chiralcel OD-RH) was selected to separate ORP enantiomers in reversed-phase mode, and the chromatographic conditions including the kind and content of organic modifier, the concentrations and types of buffer solution, and the pH of the buffer solution were optimized. Then, different extraction techniques including liquid–liquid extraction, solid-phase extraction, and protein precipitation were investigated in order to obtain better recovery efficiency, lower matrix effects, more convenient operation, and lower costs. Besides, the elution order and absolute configurations of ORP enantiomers on the Chiralcel OD-RH column could be determined by contrasting the theoretical electronic circular dichroism with the experimentally determined circular dichroism spectrum. On this basis, an HPLC-MS/MS method with multiple reaction monitoring (MRM) mode was developed for determining ORP enantiomers in rat plasma. The method was so sensitive that the LLOQ could reach 0.1 ng mL^{-1}, and a short analysis time (7 min) could be obtained. And the method was more sensitive, lower-cost, and lower power consumption than the previous report.[10] This method is reproducible and has been applied to the study of stereoselective pharmacokinetics of ORP enantiomers in rats after oral administration of ORP racemate for the first time. Taking into account the success of enantioseparation and enantioselective pharmacokinetic study for ORP, it was expected that this study would provide available information for the stereoselective study of the enantiomers, and even the further development of the individual enantiomers.

2. Experimental

2.1. Chemicals and reagents

Standards of racemic orphenadrine hydrochloride (ORP) (≥98.0% purity) and diphenhydramine hydrochloride (≥98.0% purity, Internal standard, IS) were purchased from Aladdin (Shanghai, China). MS-grade methanol (MeOH), acetonitrile (ACN), isopropanol (IPA), and ethanol (EtOH) were supplied by Sigma Aldrich (Beijing, China). All other reagents were of analytical grade and supplied by Yuwang Industrial Co., Ltd (Shandong, China). The water used was purified by a Milli-Q academic water purification system (Millipore, MA, USA).

2.2. Chiral HPLC-MS/MS conditions

The chromatographic analysis was carried out on a Waters Acquity™ UPLC system (Waters Corp., Milford, MA, USA), consisting of an Acquity™ UPLC quaternary pump solvent management system, an Acquity™ UPLC auto-sampler, and a thermostatic column compartment. The enantioseparation of ORP was performed on a Chiralcel OD-RH (150 mm × 4.6 mm i.d., 5 μm) column which was supplied by Daicel Chiral Technologies Co., Ltd (Tokyo, Japan). The optimized enantiomeric separation was obtained with the mobile phase consisting of 30 mM ammonium bicarbonate buffer at pH 9.0 and ACN (20 : 80, v/v), with a flow rate of 0.6 mL min^{-1}. The column temperature and auto-sampler temperature were set at 20 °C and 4 °C, respectively. The injection volume was 10 μL.

The Micromass Quattro micro™ atmospheric pressure ionization mass spectrometer was equipped with an electrospray ionization source (ESI), operating in positive ion mode with multiple reaction monitoring modes (MRM). The optimal MS parameters were set as follows: capillary voltage of 3.0 kV; source temperature of 150 °C; desolvation temperature of 500 °C; desolvation gas (nitrogen) flow of 1000 L h^{-1}; collision gas (argon) flow of 0.12 mL min^{-1}; nebulizer gas pressure of 7.0 bar. For ORP, the cone voltage (CV) was set at 25 V and the ion pair transitions of m/z 270.0 > 181.1 and m/z 270.0 > 165.1 were used for quantification and identification, respectively. The corresponding collision energy (CE) was 10 eV and 40 eV, respectively. For diphenhydramine (IS), the cone voltage (CV) was set at 12 V and the ion pair transitions of m/z 256.2 > 167.1 and m/z 256.2 > 152.0 were used for quantification and identification, respectively. The corresponding CE was 12 eV and 32 eV, respectively.

2.3. Preparation of standard and quality control solutions

Stock standard solutions of racemic ORP and IS were prepared in MeOH at the concentration level of 1.0 mg mL^{-1}. The stock solution of racemic ORP was further diluted in MeOH to obtain a series of working standard solutions ranging from 1.0 to 500.0 ng mL^{-1} for each enantiomer. The IS stock solution was subsequently diluted to the concentration of 25.0 ng mL^{-1} of IS working solution. Calibration standards were prepared by spiking 20 μL of appropriate rac-ORP working standard solutions and 20 μL of IS working solution into 100 μL of blank rat plasma. Then, the final plasma concentrations for each ORP enantiomer were 0.1, 0.5, 1.0, 5.0, 10.0, 20.0, and 50.0 ng mL^{-1}. Quality control (QC) samples were prepared at 0.3, 3.0, and 30.0 ng mL^{-1} for each enantiomer by the same steps. All the working standard solutions for ORP and IS were freshly prepared when needed and stored at 4 °C in a refrigerator.

2.4. Sample preparation

100 μL plasma sample was transferred into a 2.0 mL Eppendorf tube, followed by the addition of 20 μL IS working solution and 20 μL MeOH. After vortex mixing with 100 μL of 1 M sodium hydroxide solution for 30 s, the mixed sample was extracted with 1.0 mL ethyl acetate by vortexing for 5 min and centrifuged at 10 000 rpm for 10 min. Following centrifugation, the organic layer was pipetted to another Eppendorf tube and evaporated to dryness with a gentle stream of nitrogen at 40 °C. The residue was reconstituted with 200 μL MeOH and filtered through a 0.22 μm nylon syringe filter (Beijing Sunrise T&D Company, China). Finally, 10 μL of the subsequent filtrate was injected into the analytical system for LC-MS/MS analysis.

2.5. Method validation

The HPLC-MS/MS method was validated according to the US Food and Drug Administration (FDA) guidelines for bioanalytical method validation and included determination of selectivity, carryover effect, linearity, the lower limit of quantitation (LLOQ), precision, accuracy, recovery, matrix effect, and stability.[35]

The method selectivity was investigated with respect to the possible interference of endogenous biological matrix compounds in the *R*/*S*-ORP and IS determinations. Therefore, the MRM chromatograms of samples from blank rat plasma were compared to those obtained from the blank plasma spiked with ORP enantiomers at LLOQ level (0.1 ng mL^{-1}) and IS (5.0 ng mL^{-1}), and from the actual plasma samples collected at 1 h after oral administration of 10 mg kg^{-1} racemic ORP. The plasma samples were from six different rats by the same sample extraction process. The carryover effect was assessed by injecting the blank sample just after the sample of the upper limit of quantification (ULOQ, 50.0 ng mL^{-1}). The response values of interference components and carryover at the retention time of the analytes should be lower than 20% of the LLOQ peak area and 5% of the IS peak area, respectively.

The calibration curves in seven concentration levels prepared in triplicate were constructed on three different days for the determination of linearity. Plasma calibration curves were created by plotting the peak area ratios of the analyte to IS (Y) against the concentration of the analyte (X) with $1/x^2$ weighting. The lower limit of quantification (LLOQ) was established as the lowest concentration on the standard curve with a signal-to-noise ratio (S/N) $\geq$ 10. The detection was repeated six times, with accuracy (relative error, RE) and precision (relative standard deviation, RSD) below 20%.

Precision was evaluated as repeatability (intra-day) by measuring the concentrations of six replicates of low QC (LQC, 0.3 ng mL^{-1}), medium QC (MQC, 3.0 ng mL^{-1}), and high QC (HQC, 30.0 ng mL^{-1}), and the LLOQ (0.1 ng mL^{-1}) samples in one day, and as intermediate precision (inter-day) on three consecutive days. Accuracy was verified by comparing the experimental and nominal concentration for each sample from precision determinations. The acceptability criteria for accuracy and precision were ±15% of deviation for QC determinations and ±20% of deviation for the LLOQ.

The extraction recoveries of ORP enantiomers and IS were evaluated by comparing the peak areas obtained from pre-extracted plasma samples spiked with analytes and post-extracted plasma samples spiked with analytes. The matrix factors of ORP and IS were determined by contrasting the peak areas of analytes in the blank processed matrix with those in the neat standard solution. Then, the IS-normalized matrix factor (NMF) was calculated by comparing the matrix factors of IS and ORP. And the RSD of NMF should not be more than 15%. All tests were conducted at three QC concentrations in six replicates.

The stability of racemic ORP and IS under various storage conditions was determined by two-level QC samples (LQC and HQC) including short-term stability at room temperature (25 °C) for 8 h, post-preparative stability at the autosampler (4 °C) for 24 h, freeze–thaw stability at −20 °C for three cycles, and long-term stability at −80 °C for 30 days. Six replicates per condition were analyzed, and the accuracy (RE) and precision (RSD) were expected to be less than 15%.

2.6. Enantioselective pharmacokinetic study

Six male Sprague-Dawley (SD) rats, with the weight of 200–220 g, specific-pathogen-free grade, were purchased from the Experimental Animal Center of Shenyang Pharmaceutical University (License No. SCXK-Liao-2015-0001, Shenyang, China). The rats were allowed to adapt for seven days under controlled conditions (temperature: 25 °C, a standard diet, free access to water) and fasted 12 h before the experiment. Following the oral administration of 10 mg kg^{-1} of racemic ORP to six SD rats, 0.3 mL blood samples were collected from the orbital venous plexus into the coated 1.5 mL of heparinized polypropylene centrifuge tubes at 0 (pre-dose), 0.25, 0.5, 0.75, 1.0, 1.5, 2.0, 3.0, 4.0, 6.0, 8.0, and 24.0 h, respectively. Obtained blood samples were immediately centrifuged at 3500 rpm for 10 min, and then drug-containing plasma was collected and stored at −20 °C until analysis. All animal procedures were carried out in accordance with the Guidelines for Care and Use of Laboratory Animals of Shenyang Pharmaceutical University and approved by the Animal Ethics Committee of Shenyang Pharmaceutical University.

2.7. Pharmacokinetic data analysis

The concentrations of ORP enantiomers in the plasma were determined by the accompanying calibration curve of each analysis batch. Pharmacokinetics parameters including the elimination half-life ($t_{1/2}$), the area under the drug concentration–time curve (AUC), apparent volume of distribution (V_d), mean residence time (MRT), the variance of residence time (VRT), and body clearance (CL) were calculated using the DAS Software (Version 2.0, Shanghai, China). The maximum concentration (C_{max}) and time to reach the maximum concentration (T_{max}) were intuitively observed based on the concentration–time curve. All data are presented as the mean ± standard deviation (SD). The statistical analysis of the Student's *t*-test was performed to evaluate the difference of pharmacokinetic parameters between two ORP enantiomers by using SPSS Statistics 19 Software (Chicago, USA).

3. Results and discussion

3.1. Elution order and absolute configuration determination of ORP enantiomers

The absolute configurations and elution order of ORP enantiomers were determined by the comparison of the theoretical electronic circular dichroism (ECD) with the experimentally determined CD spectrum. As the enantiomers of ORP were difficult to procure, we prepared a single ORP enantiomer using a Shimadzu LC-10A HPLC system equipped with an LC-10AT pump, a fixed injection-loop of 20 μL, and an SPD-10A UV-vis Detector. In this work, the individual enantiomers of rac-ORP were successively collected by semi-preparative reversed-phase liquid chromatography (Shimadzu, Japan) under the optimized enantioseparation conditions in Section 2.2. Then, the MeOH solutions of the first and second eluted enantiomer were distinguished by MOS-450 CD Spectrometer (Bio-Logic, France). As depicted in Fig. 2, the first eluted peak (Peak 1, red line) showed a positive cotton effect at 203 and 226 nm, whilst the second eluted peak (Peak 2, blue line) showed a negative cotton effect, and the response values of the two peaks were the same. Moreover, for each enantiomer of ORP, the experimental CD spectrum and the calculated ones using the time-dependent density functional theory (DFT) method were compared. The calculated ECD spectrum of the *R*-isomer showed positive cotton effects (red dashed line), which was consistent with the experimental CD spectra of the first eluted enantiomer (Peak 1). In contrast, the calculated ECD spectrum of the *S*-isomer showed negative cotton effects (blue dashed line), which corresponded to the second eluted enantiomer (Peak 2). Base on the above evidence, the absolute configurations of the first and second eluted enantiomer were established to be *R* and *S*, respectively.

3.2. Optimization of chromatographic conditions

Chiral separation of rac-ORP was investigated by HPLC in reversed-phase mode. The effect of chiral columns, the type and content of organic modifier, the kind and concentration of buffer solution, and the pH of the buffer solution on chiral separation was investigated. The preliminary work was devoted to the enantioseparation of ORP on four polysaccharide-based columns (Chiralpak IA, Chiralpak IC, Chiralpak ID, and Chiralcel OD-RH) under the reversed-phase mode. On the four tested columns, satisfactory enantioselectivity for rac-ORP was obtained by using a Chiralcel OD-RH column. The other three columns showed poor chiral recognition capability towards the ORP enantiomers although different mobile phase compositions and additives were trialed. Therefore, the Chiralcel OD-RH column was finally chosen for the following study.

The mobile phase plays a crucial role in the enantioseparation based on the efficiency, retention behavior, and resolution value (R_s) of enantiomers. In our experiments, the influence of concentrations and types of buffer solution such as ammonium carbonate, ammonium bicarbonate, and ammonium acetate on enantioseparation efficiency were individually investigated. It was found that the ammonium bicarbonate buffer solution could provide the best resolution (R_s = 2.254) for ORP enantiomers compared with the ammonium carbonate (R_s = 2.192) and ammonium acetate (R_s = 1.294). And the solution of ammonium bicarbonate gave rise to better peak shapes as well as lower column pressure. Based on this, the organic modifier (ACN) admixed with ammonium bicarbonate buffer (pH 9.0) in several concentrations was tried as a mobile phase; with the increase of buffer concentration from 5 to 30 mM, the chiral resolution of ORP showed a tendency to increase (R_s from 1.861 to 3.511). The impact of buffer solution pH (a binary mixture of 30 mM ammonium bicarbonate buffer with ACN) on the retention and selectivity was studied in the range from pH 7.0 to 9.0. As depicted, increasing the buffer pH from 7.0 to 9.0, the resolution and separation factor (α) was increased and the retention capacity (k_1) decreased (Table 1). The crucial step to improve the enantioseparation is the choice of a suitable organic modifier. In our study, the chiral separation ability of Chiralcel OD-RH toward ORP was evaluated with mobile phases containing 95% (v/v) MeOH, 80% ACN, and 85% EtOH in 30 mM ammonium bicarbonate buffer (pH = 9.0). The results showed that the use of ACN (R_s = 3.557) as the organic modifier provided better resolution for ORP than that using MeOH (R_s = 1.738) or EtOH (R_s = 1.701). The effect of the contents of ACN on the chiral separation of ORP enantiomers was evaluated herein. From Table 2, enantioseparation parameters of the studied compounds including k_1, α, and R_s were all increased with the decrease of the content of organic modifiers. Therefore, as an integrated strategy taking into account R_s, retention time, and peak shape, Chiralcel OD-RH with the mobile phase of ammonium bicarbonate buffer (30 mM, pH 9.0)/ACN (20/80, v/v) was selected as the optimized enantioseparation conditions.

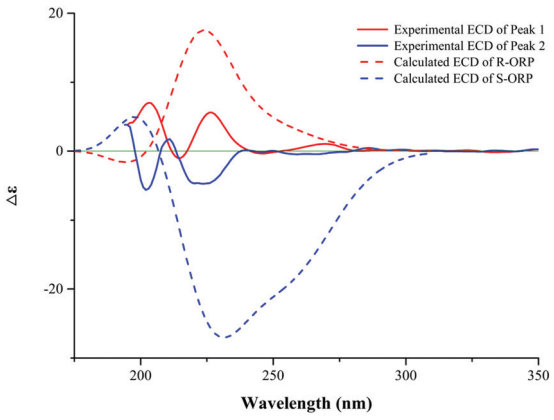

Fig. 2 Calculated and experimental ECD spectra of *R*-ORP and *S*-ORP.

Table 1 Effect of the pH of the buffer solution on the chiral separation of ORP enantiomers. Mobile phase: 30 mM ammonium bicarbonate buffer/ACN (20 : 80, v:v)

The pH of the buffer solution	k_1	α	R_s
9.0	0.554	1.365	3.554
8.5	0.918	1.315	2.864
8.0	0.948	1.275	2.548
7.5	1.005	1.268	2.378
7.0	1.168	1.219	2.107

Table 2 Effect of the content of ACN on the chiral separation of ORP enantiomers. Mobile phase: 30 mM ammonium bicarbonate buffer (pH 9.0)/ACN

The content of ACN (%)	k_1	α	R_s
10	0.471	1.347	2.219
20	0.639	1.403	3.562
30	1.173	1.425	4.123
40	1.984	1.441	5.021
50	2.758	1.447	6.127

3.3. Optimization of mass spectrometry conditions

The study was operated in positive ESI mode as it gave considerably higher signal intensities for ORP enantiomers and IS compared to the negative mode. MS/MS with MRM mode was used to analyze ORP enantiomers and IS because it is selective and sensitive. The analytes produced protonated molecular ions $[M + H]^+$ as the major species. For two MRM transitions, the most sensitive transition was used for quantification, while the other transition was used for confirmation. Collision energy and other parameters were investigated and adjusted using an optimizer program to achieve the highest possible MS response of the analytes.

3.4. Optimization of sample preparation

A suitable pretreatment technique can not only obtain optimal recovery and good reproducibility but also effectively reduce the impact of coexisting interferents, which is further helpful to prolong the life of a chiral chromatographic column. In our study, different extraction techniques including liquid–liquid extraction (LLE), solid-phase extraction (SPE), and protein precipitation (PPT) were investigated for removing proteins in plasma, reducing the matrix effect and ion interference in LC-MS/MS analysis. As shown in Fig. 3B, different precipitants were used for the extraction of ORP from rat plasma such as ACN, MeOH, IPA, and acetone (ACE). The recovery could reach 95% with ACN and MeOH as the precipitant to remove the protein of plasma. However, PPT is a nonselective purification means, which can introduce a large number of endogenous components into the chiral column, potentially causing its damage. Hence, the further optimization of sample preparation was investigated using LLE and SPE.

The SPE procedure was performed on three SPE cartridges including a Cleanert C18 cartridge (500 mg, 3 mL), Cleanert NH_2 cartridge (500 mg, 3 mL), and Cleanert PCX cartridge (500 mg, 3 mL). For the reversed-phase cartridge (Cleanert C18 and NH_2), 2 mL water was used as the washing solution and elution was carried out by 2 mL MeOH. The results showed that poor recovery ($<50\%$) was obtained for ORP enantiomers. It has been reported that Cleanert PCX, which would provide both reversed-phase and cationic exchange mechanisms, could be suitable for the extraction of alkaline compounds.[36,37] Thus, Cleanert PCX was also attempted in this study. After the loading and washing procedure, ORP was eluted with 2 mL of 5%

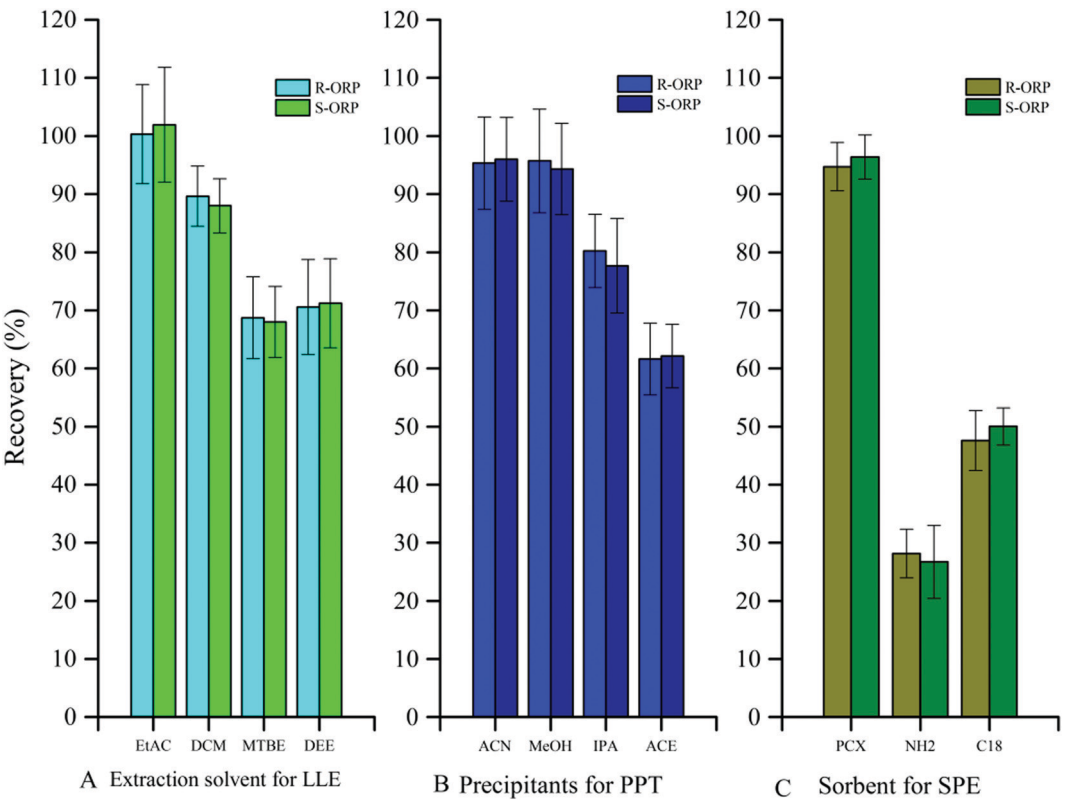

Fig. 3 Effect of the extraction solvent for LLE (A), types of precipitant for PPT (B), and sorbent for SPE (C) on the recoveries of the analytes (n = 5). Experimental conditions: (A) the volume of the solvent, 1 mL; (B) the volume of the precipitants, 2 mL.

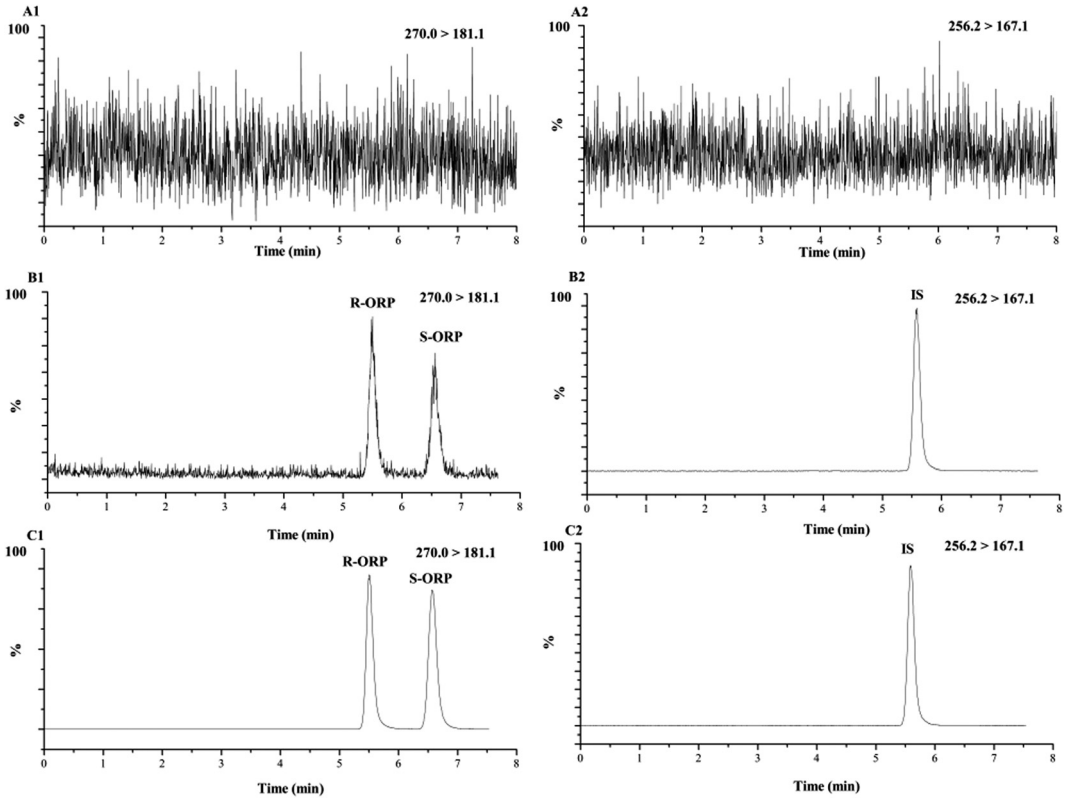

Fig. 4 Representative MRM chromatograms of *R*-ORP, *S*-ORP, and IS. (A) A blank plasma sample; (B) a blank plasma spiked with racemic ORP at the LLOQ level; (C) a plasma sample obtained at 1 h after a single dose of 10 mg kg^{-1} racemic ORP.

ammonium hydroxide in MeOH. It was found that SPE with the Cleanert PCX cartridge could provide satisfactory recovery (>90%) for ORP enantiomers (Fig. 3C).

In the optimization of LLE, several solvents such as dichloromethane (DCM), diethyl ether (DEE), ethyl acetate (EtAc), and methyl *tert*-butyl ether (MTBE) were evaluated. In comparison with other extraction agents, EtAc and DCM were more effective in extracting the ORP from plasma. As shown in Fig. 3A, when MTBE and DEE were used as extraction solvent, the recovery of ORP was lower than 70%, while recovery above 85% could be obtained using EtAc and DCM. And EtAc provided higher recovery (>95%) than DCM. To sum up, LLE with EtAc as the extraction solvent was finally chosen for the experiments, because of not only its simpler and more convenient operation but also lower costs than SPE, especially considering the application of the method in pharmacokinetic studies, for which many samples are required.

3.5. Method validation

3.5.1. Selectivity and carryover effect. Representative HPLC-MS/MS chromatograms of *R*-ORP, *S*-ORP, and IS are shown in Fig. 4. The retention time was approximately 5.55 min for *R*-ORP, 6.56 min for *S*-ORP, and 5.58 min for the IS. Due to the high selectivity and sensitivity of the method, no endogenous components interfered with the ORP enantiomers and IS. Meanwhile, no carryover effect of ORP enantiomers and IS was observed in the chromatograms acquired during the injection of blank plasma samples after successive injections of the highest concentration of the calibration standards (50.0 ng mL^{-1}).

Table 3 The accuracy, precision, extraction recovery, and matrix effect of ORP enantiomers in rat plasma

Analytes	Nominal concentration (ng mL^{-1})	Intra-day (n = 6)		Inter-day (n = 18)		Extraction recovery (n = 6)		Matrix effect (n = 6)	
		RSD (%)	RE (%)	RSD (%)	RE (%)	Mean ± SD (%)	RSD (%)	Mean ± SD (%)	RSD (%)
R-ORP	0.1	9.20	11.22	9.04	10.45	—	—	—	—
	0.3	3.65	9.03	3.17	8.18	102.51 ± 3.41	3.33	105.04 ± 4.08	3.88
	3	1.58	9.07	1.68	9.26	91.22 ± 6.46	7.08	106.53 ± 3.49	3.28
	30	1.61	7.25	1.17	5.29	107.18 ± 5.90	5.50	107.79 ± 4.39	4.07
S-ORP	0.1	7.72	10.07	7.15	10.28	—	—	—	—
	0.3	4.08	10.82	4.26	9.26	105.21 ± 2.95	2.80	105.73 ± 3.56	3.36
	3	1.95	11.47	1.04	9.37	92.28 ± 6.19	6.71	107.05 ± 3.38	3.16
	30	1.38	7.18	1.02	6.19	108.29 ± 5.21	4.81	107.41 ± 2.52	2.35

Table 4 Stability of ORP enantiomers in rat plasma samples at different conditions (n = 6)

		Room temperature, 8 h		Three freeze–thaw cycles		Autosampler tray, 4 °C, 24 h		−80 °C, 30 days	
Analytes	Concentrations (ng mL^{-1})	RE (%)	RSD (%)	RE (%)	RSD (%)	RE (%)	RSD (%)	RE (%)	RSD (%)
R-ORP	0.3	12.05	3.16	4.32	3.51	11.82	1.42	8.37	3.55
	30	−11.15	9.46	11.80	2.51	11.93	2.55	9.66	8.67
S-ORP	0.3	10.91	2.96	2.78	2.82	10.11	1.47	9.04	4.01
	30	−10.60	10.44	10.25	2.46	11.72	3.61	8.29	9.37

3.5.2. Linearity and lower limit of quantitation (LLOQ). The calibration curves of ORP enantiomers in the plasma were evaluated by linear regression analysis with $1/x^2$ weighting. The regression equations of the calibration curves were as follows: $Y = (0.144 \pm 0.00446)\,X + (0.061 \pm 0.00140)$ for *R*-ORP and $Y = (0.152 \pm 0.00427)\,X + (0.056 \pm 0.00151)$ for *S*-ORP. The curves showed good linearity ($r > 0.996$) for all of the matrices in the range of 0.1–50.0 ng mL^{-1}. The LLOQ of each ORP enantiomer was 0.1 ng mL^{-1} for the plasma with acceptable accuracy and precision (Table 3).

3.5.3. Accuracy and precision. Table 3 shows the results of intra-day and inter-day precision and accuracy for *R*-ORP and *S*-ORP in rat plasma. The intra-day and inter-day precision (RSD) were less than 9.20%, while the accuracy (RE) ranged from 5.29% to 11.47%, indicating satisfactory precision and accuracy of the assay.

3.5.4. Extraction recovery and matrix effect. The extraction recoveries of *R*-ORP were 102.51 ± 3.41%, 91.22 ± 6.46%, and 107.18 ± 5.90% at three concentrations of 0.1, 3.0, and 30.0 ng mL^{-1}, respectively, while the recoveries of *S*-ORP were 105.21 ± 2.95%, 92.28 ± 6.19%, and 108.29 ± 5.21%, respectively, with no significant variation among the three concentrations (RSD < 7.08%). The mean extraction recovery of IS was 103.29 ± 9.69%. The results demonstrated the reproducibility and consistency of the extraction recovery of ORP enantiomers. The matrix effects of the ORP enantiomers were 100.96–112.18%, indicating an acceptable matrix effect for *R*-ORP and *S*-ORP in the biological samples. The results are shown in Table 3.

3.5.5. Stability. An important process of bioanalytical method validation is stability assessment. The stability of *R*-ORP and *S*-ORP was studied through analysis of LQC and HQC plasma samples of the two enantiomers after the application of the different storage conditions. As presented in Table 4, the calculated accuracies (RE) were within the range of −11.15 to 12.05% for *R*-ORP and the range of −10.60 to 10.91% for *S*-ORP of the nominal concentrations which lies within the acceptable range. These results demonstrate that the ORP enantiomers could maintain stability under experimental routine conditions of storage and analysis of the biological samples.

3.6. Application to an enantioselective pharmacokinetic study

The validated bioanalytical method was successfully applied to the investigation of the enantioselective pharmacokinetics of ORP enantiomers after the administration of a single oral dose of 10 mg kg^{-1} racemic ORP to six SD rats. As far as we know, this investigation is the first time that the HPLC-MS/MS technique has been utilized to quantify the concentrations of *R*-ORP and *S*-ORP in rat plasma and applied to an enantioselective pharmacokinetic study. The mean plasma concentration-time profiles of *R*-ORP and *S*-ORP are presented in Fig. 5, and the pharmacokinetic parameters are summarized in Table 5. The pharmacokinetic parameters were compared by paired sample *T*-tests. Differences in parameters were considered as statistically significant at $P < 0.05$.

As can be seen in Fig. 5, the concentrations of the two ORP enantiomers both rapidly increased following oral absorption, and reached the maximum plasma concentration after 1.0 h. The plasma concentration of *S*-ORP was consistently higher than that of *R*-ORP after oral administration of *rac*-ORP. By comparing the drug concentration-time curves of the *R*/*S*-ORP enantiomers more precisely, it was found that the mean C_{max} value of *S*-ORP was 1.26 times greater than that of *R*-ORP, and the AUC_{0-t} was 1.2-fold higher than that of *R*-ORP. Besides, the results indicated that significant differences could be observed between the two enantiomers with higher $t_{1/2}$, CL, V_d, MRT_{0-t}, and VRT_{0-t} for *R*-ORP than that obtained for *S*-ORP. These significant stereoselectivity data were first analyzed and observed in our study.

To some extent, the obvious differences in plasma levels may be attributed to the conversion between the two enantiomers *in vivo*.[38–42] However, thus far, we could not address this problem with the limited access to a single enantiomer. Besides, the previous study revealed the high enantioselectivity of the binding of ORP enantiomers to serum albumin,[11,27] which might partly provide an explanation for the observed pharmacokinetic differences of

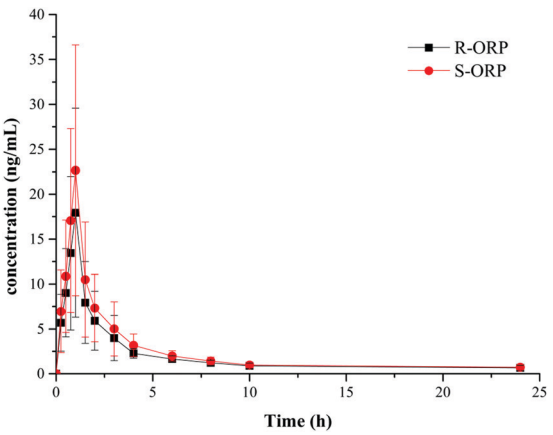

Fig. 5 Mean plasma drug concentration-time curves of *R*-ORP and *S*-ORP in rats after oral administration of 10 mg kg^{-1} racemic ORP. Each point represents the mean ± SD.

Table 5 Pharmacokinetic parameters (mean ± SD) of *R*-ORP and *S*-ORP after oral administration of racemic ORP to six rats

	ORP (10 mg kg^{-1})	
Parameters	*R*-ORP	*S*-ORP
T_{max} (h)	1.0 ± 0.00	1.0 ± 0.00
C_{max} (ng mL^{-1})	17.94 ± 11.62	22.66 ± 13.96
AUC_{0-t} (ng h mL^{-1})	46.99 ± 19.41	57.21 ± 25.35
$AUC_{0-\infty}$ (ng h mL^{-1})	52.62 ± 25.34	58.47 ± 24.73
$t_{1/2}$ (h)	8.35 ± 4.79	4.52 ± 1.99
CL (L h^{-1} kg^{-1})	198.59 ± 80.80	179.19 ± 74.98
V_d (L kg^{-1})	2299.76 ± 817.13	1349.63 ± 847.00
MRT_{0-t} (h)	6.03 ± 1.35	5.70 ± 1.32
VRT_{0-t} (h)	46.46 ± 11.62	43.58 ± 11.95

C_{max}, the maximum plasma drug concentration; T_{max}, time to reach the maximum plasma drug concentration; AUC_{0-t}, area under the drug concentration–time curve to the last measurable concentration; $AUC_{0-\infty}$, area under plasma drug concentration–time curve to infinity; $t_{1/2}$, elimination half-life; CL, the body clearance; MRT_{0-t}, the mean residence time; VRT_{0-t}, the variance of residence time.

R/*S*-ORP in our study. Further research should be performed on the enantioselective absorption, distribution, metabolism, and excretion of ORP enantiomers *in vivo*, thereby ascertaining suitable clinical administration.

4. Conclusions

The first chiral reversed-phase mode HPLC-MS/MS method for the determination of ORP enantiomers in rat plasma was developed and validated. The enantioseparation was performed on a Chiralcel OD-RH column with enough resolution (R_s = 3.562) and a short analysis time (7 min). The LLOQ of each ORP enantiomer was demonstrated to be 0.1 ng mL^{-1}, which was significantly lower than the previous report (1.0 ng mL^{-1}).[10] After the method validation, the developed method was applied to the enantioselective pharmacokinetic study of ORP enantiomers after oral administration of 10 mg kg^{-1} racemic ORP to SD rats. It was revealed that there were significant differences between the two enantiomers of ORP in some important pharmacokinetic parameters, indicating the enantioselective pharmacokinetic behavior of ORP in rats.

Abbreviations

MRM	Multiple reaction monitoring
C_{max}	The maximum plasma drug concentration
T_{max}	Time to reach the maximum plasma drug concentration
AUC	Area under the drug concentration–time curve
$t_{1/2}$	Elimination half-life
CL	The body clearance
V_d	Apparent volume of distribution
MRT	The mean residence time
VRT	The variance of residence time

CRediT authorship contribution statement

Yanru Liu: Conceptualization, Methodology, Investigation, Writing – Original draft preparation. Yushan Ding: Software, Investigation, Validation. Yongbo Song: Conceptualization, Software, Writing – Review & Editing. Xingjie Guo: Conceptualization, Resources, Writing – Review & Editing.

Funding

This research did not receive any specific grant from funding agencies in the public, commercial, or not-for-profit sectors.

Conflicts of interest

There are no conflicts to declare.

References

1 B. Ren, B. Jia, X. Zhang, J. Wang, Y. Li, H. Liang and H. Liang, *Chemosphere*, 2021, **267**, 128872.
2 M. Bao, J. Li, H. Chen, Z. Chen, D. Xu and Y. Wen, *Sci. Total Environ*, 2021, **757**, 143759.
3 C. Ji, J. Magnuson, W. Zhang and M. Zhao, *J. Hazard. Mater.*, 2021, **403**, 123893.
4 Y. Zhao and W. Pritts, *J. Chromatogr. A*, 2001, **1156**, 228–235.
5 M. Khan, B. Viswanathan, D. Rao and R. Reddy, *J. Chromatogr. B*, 2007, **846**, 119–123.
6 Q. Tian, Z. Zhou, C. Lv and J. Yang, *Anal. Methods*, 2012, **4**, 2307–2317.
7 M. Li, J. Zhang, S. Ma, Z. Jiang, X. Di and X. Guo, *New J. Chem.*, 2020, **44**, 5819–5827.
8 J. Du, Y. Zhang, Y. Chen, D. Liu, X. Chen and D. Zhong, *J. Chromatogr. B*, 2014, **965**, 224–230.
9 K. Cheah, K. Mah, L. Pang, S. Ng, J. Wong, S. Tan, H. Tan and K. Yuen, *BMC Pharmacol. Toxicol.*, 2020, **21**, 45.
10 S. Lee, H. Oh, J. Kim, Y. Kim, C. Moon and E. Lee, *J. Chromatogr. B*, 2006, **839**, 118–123.
11 M. Martinez-Gomez, R. Villanueva-Camanias, S. Sagrado and M. Medina-Hernandez, *Electrophoresis*, 2007, **28**, 3056–3063.
12 M. Martinez-Gomez, S. Sagrado, R. Villanueva-Camanias and M. Medina-Hernandez, *Anal. Chim. Acta*, 2007, **592**, 202–209.
13 Y. Tang, H. Wu, S. Wu, S. Chen and H. Kou, *J. Microcolumn Sep.*, 2000, **12**, 366–370.
14 L. Asensi-Bernardia, L. Escuder-Gilaberta, Y. Martín-Bioscaa, S. Sagradoa and M. Medina-Hernández, *Biomed. Chromatogr.*, 2014, **28**, 120–126.
15 A. Stalcup and K. Gahm, *Anal. Chem.*, 1996, **68**, 2248–2250.
16 B. Koppenhoefer, U. Epperlein, X. Zhu and B. Lin, *Electrophoresis*, 1997, **18**, 924–930.
17 B. Koppenhoefer, U. Epperlein, R. Schlunk, X. Zhu and B. Lin, *J. Chromatogr. A*, 1998, **793**, 153–164.
18 Y. Liu, B. Zhu, M. Xue, Z. Jiang and X. Guo, *Microchem. J.*, 2020, **156**, 104989.

19 B. Zhu, M. Xue, B. Liu, Q. Li and X. Guo, *J. Pharm. Biomed.*, 2019, **176**, 112803.
20 B. Mondal, *Saudi Pharm. J.*, 2020, **28**, 325–328.
21 X. Zhang, Y. Bao, K. Huang, K. Barnett-Rundlett and D. Armstrong, *Chirality*, 2010, **22**, 495–513.
22 Y. Yang, J. W. Hu, H. Fang, X. B. Hou, Z. Hou, L. H. Sang and X. Y. Yang, *J. Chromatogr. A*, 2020, **1632**, 461598.
23 H. Y. Wang, J. W. Shen, Y. Wu, X. Sun, Y. Zhou and Y. Ke, *J. Chromatogr. A*, 2020, **1632**, 461608.
24 L. Peng, S. Jayapalan, B. Chankvetadze and T. Farkas, *J. Chromatogr. A*, 2010, **1217**, 6942–6955.
25 G. Hellinghausen, D. Roy, J. Lee, Y. Wang, C. Weatherly, D. Lopez, K. Nguyen, J. Armstrong and D. Armstrong, *J. Pharm. Biomed.*, 2018, **155**, 70–81.
26 K. Kumar, S. Meyyanathan and B. Gowramma, *J. Pharm. Sci.*, 2016, **43**, 127–134.
27 M. Martinez-Gomez, R. Villanueva-Camanas, S. Sagrado and M. Medina-Hemandez, *Electrophoresis*, 2007, **28**, 2635–2643.
28 S. Boltia1, A. Soudi, E. Elzanfaly and H. Zaazaa, *J. Chromatogr. Sci.*, 2019, 1–11.
29 S. Selkirk, A. Fell, G. Smith and J. Miller, *J. Chromatogr. A*, 1984, **288**, 431–444.
30 J. Labout, C. Thijssen, G. Keijser and W. Hespe, *Eur. J. Chlin. Pharmacol.*, 1982, **21**, 343–350.
31 J. Labout, C. Thijssen and W. Hespe, *J. Chromatogr. A*, 1977, **144**, 201–208.
32 M. Katselou, S. Athanaselis, P. Nikolaou, A. Dona, C. Spiliopoulou and I. Papoutsis, *J. Pharm. Biomed.*, 2017, **145**, 765–772.
33 M. Katselou, S. Athanaselis, P. Nikolaou, S. Qammaz, A. Dona, C. Spiliopoulou and I. Papoutsis, *Biomed. Chromatogr.*, 2018, 32.
34 R. Cunha, M. Ribeiro, R. Munoz and E. Richter, *J. Sep. Sci.*, 2018, **40**, 1815–1823.
35 Bioanalytical Method Validation Guidance for Industry, Center for Drug Evaluation and Research of the U.S. Department of Health and Human Services Food and Drug Administration, 2018.
36 D. Chen, Y. Zhao, H. Miao and Y. Wu, *Talanta*, 2015, **134**, 144–152.
37 Y. Ji, Y. Wang, T. Fu, S. Ma, Y. Qi, J. Si, D. Sun and Y. Liao, *Int. J. Environ. An. Ch.*, 2019, **99**, 1090–1102.
38 B. Du, L. Pang, Y. Yang, G. Shen and Z. Zhang, *J. Chromatogr. B*, 2014, **951–952**, 143–148.
39 Y. Du, L. Luo, S. Sun, Z. Jiang and X. Guo, *Anal. Bioanal. Chem.*, 2017, **409**, 6315–6323.
40 W. Hao, Y. Zhang, P. Xu, Y. Xie, W. Li and H. Wang, *Chemosphere*, 2021, **271**, 129482.
41 Z. Liu, D. Chen, J. Han, Y. Chen and K. Zhang, *Environ. Res.*, 2021, **194**, 110680.
42 H. Heep, J. Hubeli, T. Fleischmann, P. Lienemann, N. Nayyar, R. Lal and H. Kohler, *Chemosphere*, 2021, **267**, 129217.

